

Realization of a strongly interacting Bose-Fermi mixture from a two-component Fermi gas

Yong-il Shin,* André Schirotzek, Christian H. Schunck, and Wolfgang Ketterle

Department of Physics, MIT-Harvard Center for Ultracold Atoms, and Research Laboratory of Electronics, Massachusetts Institute of Technology, Cambridge, Massachusetts 02139, USA

(Dated: June 28, 2021)

We show the emergence of a strongly interacting Bose-Fermi mixture from a two-component Fermi mixture with population imbalance. By analyzing *in situ* density profiles of ${}^6\text{Li}$ atoms in the BCS-BEC crossover regime we identify a critical interaction strength, beyond which all minority atoms pair up with majority atoms, and form a Bose condensate. This is the regime where the system can be effectively described as a boson-fermion mixture. We determine the dimer-fermion and dimer-dimer scattering lengths and beyond-mean-field contributions. Our study realizes a Gedanken experiment of bosons immersed in a Fermi sea of one of their constituents, revealing the composite nature of the bosons.

PACS numbers: 03.75.Ss, 03.75.Hh, 67.60.Fp

Fermions are the fundamental building blocks of matter, whereas bosons emerge as composite particles. The simplest physical system to study the emergence of bosonic behavior is a two-component fermion mixture, where the composite boson is a dimer of the two different fermions. A dramatic manifestation of bosonic behavior is Bose-Einstein condensation, representing the low-temperature phase of a gas of bosons. One way to reveal the composite nature of the bosons is to immerse such a Bose-Einstein condensate (BEC) into a Fermi sea of one of its constituents. The degeneracy pressure due to the Pauli exclusion principle affects the structure of the composite boson, resulting in a zero-temperature quantum phase transition to a normal state where Bose-Einstein condensation is quenched.

In this paper we observe this transition experimentally. We identify the regimes where a two-component Fermi gas can be described as binary mixture of bosons and fermions, and where the composite nature of the boson becomes essential. The validity of a Bose-Fermi (BF) description requires that all minority fermions become bound as bosons and form a BEC. We determine the critical value of $1/k_{F\uparrow}a$ for the onset of superfluid behavior in the limit of large population imbalance. Here a is the fermion-fermion scattering length and $k_{F\uparrow}$ is the Fermi wave number characterizing the depth of the majority Fermi sea. Of course, for an equal mixture, the zero-temperature ground state is always a superfluid in the BEC-BCS crossover. It has been shown previously that a crossover superfluid can be quenched by population imbalance, also called the Chandrasekhar-Clogston (CC) limit of superfluidity [1, 2]. In this work we determine the critical point where superfluidity can no longer be quenched by population imbalance, i.e. the CC limit becomes 100%.

In the limit of a BF mixture [3], we observe repulsive interactions between the fermion dimers and unpaired fermions. They are parameterized by an effec-

tive dimer-fermion scattering length of $a_{\text{bf}} = 1.23(3)a$. This value is consistent with the exact value $a_{\text{bf}} = 1.18a$ which has been predicted over 50 years ago for the three fermion problem [4], but has never been experimentally confirmed. The boson-boson interactions were found to be stronger than the mean-field prediction in agreement with the Lee-Huang-Yang prediction [5].

The system for this study is a variable spin mixture of the two lowest hyperfine states $|\uparrow\rangle$ and $|\downarrow\rangle$ of ${}^6\text{Li}$ atoms (corresponding to the $|F = 1/2, m_F = 1/2\rangle$ and $|F = 1/2, m_F = -1/2\rangle$ states at low magnetic field) in an optical dipole trap as described in Refs. [1, 2]. A broad Feshbach resonance, located at 834 G [6], strongly enhances the interactions between the two spin states. The final evaporative cooling was performed at 780 G by lowering the trap depth. Subsequently, the magnetic-bias field B is adjusted to a target value with a ramp speed of ≤ 0.4 G/ms, changing the interaction strength adiabatically. At the end of the preparation, our sample was confined in an effective three-dimensional harmonic trap with cylindrical symmetry. The axial (radial) trap frequency was $\omega_z/2\pi = 22.8$ Hz ($\omega_r/2\pi = 140$ Hz).

The phase diagram for the fermion mixture was obtained from the analysis of *in situ* density profiles of the majority (spin \uparrow) and minority (spin \downarrow) components. The profiles were recorded using a phase-contrast imaging technique [2]. Under the local density approximation (LDA), low-noise column-density profiles were obtained by averaging the optical signal along equipotential lines (refer to Ref. [2] for a full description of the image processing). For typical conditions, the temperature of a sample was $T/T_{F0} \lesssim 0.05$, determined from the outer region of the cloud [2], where $T_{F0} \approx 1.0$ μK is the Fermi temperature of the majority component measured as $k_B T_{F0} = m\omega_z^2 R_\uparrow^2/2$ (k_B is the Boltzmann's constant, m is the atom mass, and R_\uparrow is the axial radius of the majority cloud).

Figure 1 displays density profiles of imbalanced Fermi

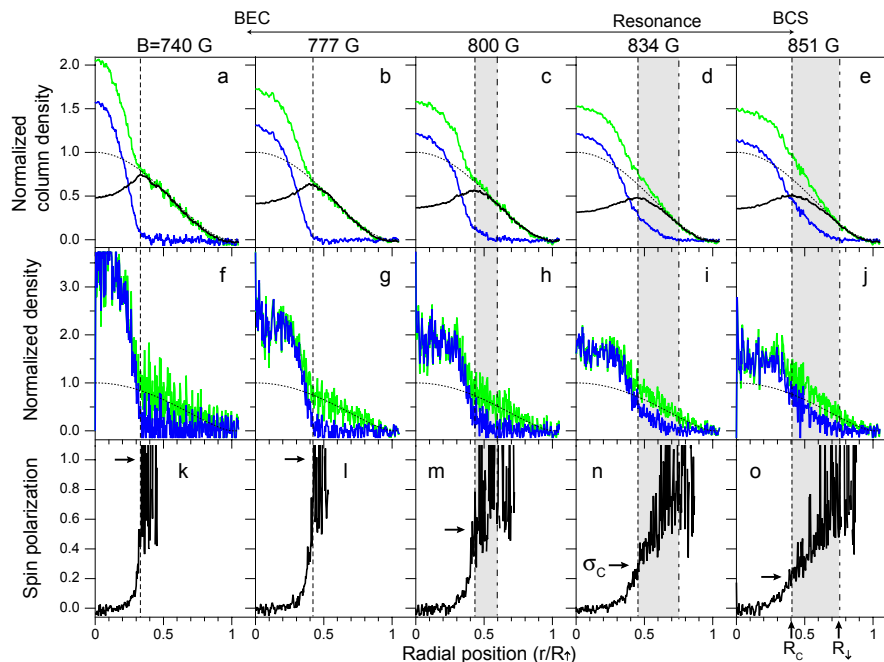


FIG. 1: (color online) Density profiles of imbalanced Fermi mixtures in a harmonic trap. The top row (a-e) shows the averaged column density profiles for various magnetic fields (green: majority, blue: minority, black: difference). The black dotted line is a zero-temperature Thomas-Fermi distribution fit to the majority wing profile ($r > R_{\downarrow}$). The middle row (f-j) and the bottom row (k-o) show the reconstructed three-dimensional density distributions and the spin polarizations obtained from the profiles in the top row. R_{\uparrow} , R_{\downarrow} (dashed dot lines), and R_c (dashed lines) are the radii of the majority cloud, the minority cloud, and the superfluid core, respectively. The critical polarizations σ_c at the phase boundary $r = R_c$ are indicated by the right arrows. The values for R_{\uparrow} (in μm), R_c/R_{\uparrow} , and $R_{\downarrow}/R_{\uparrow}$ were respectively: for (a,f,k), 381, 0.33, 0.33; for (b,g,l), 380, 0.33, 0.33; for (c,h,m), 362, 0.35, 0.59; for (d,i,n), 371, 0.44, 0.72; for (e,j,o), 367, 0.41, 0.76. $T/T_{F0} \lesssim 0.05$ and $T_{F0} \approx 1.0 \mu\text{K}$ (see the text for definitions).

mixtures for various magnetic fields, showing how the spatial structure of a trapped sample evolves in the crossover regime. Near resonance, as reported in Ref. [2], three distinctive spatial regions are identified: (I) a superfluid core, (II) an intermediate region of a partially-polarized normal (N_{pp}) phase, and (III) a fully-polarized, outer wing. The core radius R_c was determined as the peak position in the column density difference profile and the majority (minority) radius R_{\uparrow} (R_{\downarrow}) was determined from the fit of the outer region, $r > R_{\uparrow}$ ($r > R_c$) of the majority (minority) column density profile to a zero-temperature Thomas-Fermi distribution. The local spin polarization is defined as $\sigma(r) \equiv (n_{\uparrow} - n_{\downarrow})/(n_{\uparrow} + n_{\downarrow})$, where n_{\uparrow} and n_{\downarrow} are the local majority and minority density, respectively.

Further on the BEC side, the sample has a more compressed superfluid core, a narrower intermediate normal region (gray region in Fig. 1) and a higher critical spin polarization at the phase boundary $\sigma_c = \sigma(R_c)$. Eventually, when $B < 780$ G, there is no noticeable intermediate region, implying that every minority atom pairs up with a majority atom in the superfluid core. In Fig. 2 we determine the critical point for the disappearance of the partially polarized normal phase in two different ways.

Fig. 2(a) shows the phase diagram for the N_{pp} phase in the plane of interaction strength $1/k_{F\uparrow}a$ and spin polarization σ . An extrapolation of the critical line to $\sigma_c = 1$ yields $1/k_{F\uparrow,c}a = 0.74(4)$. Another implication of the absence of an N_{pp} phase is that the size of the minority cloud R_{\downarrow} approaches the radius R_c of the superfluid core. This extrapolation is conveniently done using the dimensionless parameter $\kappa = (R_{\uparrow}^2 - R_{\downarrow}^2)/(R_{\uparrow}^2 - R_c^2)$ [7], resulting in a value of $1/k_{F\uparrow,c}a = 0.71(5)$. These values are in good agreement with recent quantum Monte-Carlo (QMC) calculations [8].

The critical point marks the onset of the emergence of a BF mixture from the two-component Fermi system. One may suspect that near the critical point the equation of state of the BF mixture is complex, but we show now that a very simple equation of state is sufficient to quantitatively account for the observed profiles. Due to the external trap potential, the local chemical potential varies from zero at the edge of a cloud to a maximum value in the center. Therefore, knowledge of the three-dimensional density profiles of a single cloud is sufficient to obtain the equation of state [2, 3, 9, 10, 11].

For a zero temperature mixture of bosonic dimers with density $n_b = n_{\downarrow}$ and mass $m_b = 2m$ and un-

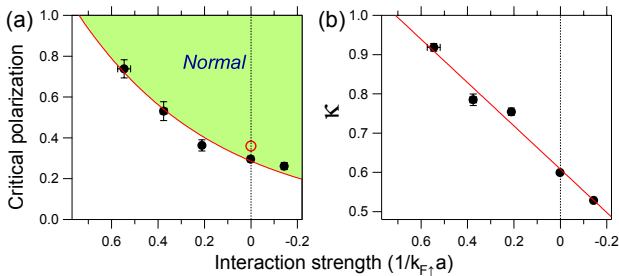


FIG. 2: (color online) Emergence of a Bose-Fermi mixture in the phase diagram for a two component Fermi gas. (a) The critical polarization σ_c as a function of the interaction strength $1/k_{F\uparrow}a$ at the phase boundary. The open circle indicates the previously measured critical value on resonance, $\sigma_{c0} = 0.36$ [2]. (b) $\kappa = (R_{\uparrow}^2 - R_{\downarrow}^2)/(R_{\uparrow}^2 + R_{\downarrow}^2)$. The red solid lines are (a) an exponential fit and (b) a linear fit to the data points. $\sigma_c = 1$ and $\kappa = 1$ (i.e. $R_{\uparrow} = R_{\downarrow}$) imply the absence of minority fermions in the normal phase. Each data point consists of nine to twenty three independent measurements and the error bars indicate only the statistical uncertainty.

paired fermions with density $n_f = n_{\uparrow} - n_{\downarrow}$ and mass $m_f = m$, the energy density \mathcal{E} can be decomposed as $\mathcal{E} = \mathcal{E}_{bb} + \mathcal{E}_{bf} + \mathcal{E}_f$, where $\mathcal{E}_{bb}(n_b)$ and $\mathcal{E}_{bf}(n_b, n_f)$ are the boson-boson and boson-fermion interaction energies, respectively, and $\mathcal{E}_f = (3/5)\alpha n_f^{5/3}$ is the kinetic energy of fermions [$\alpha = (6\pi^2)^{2/3}\hbar^2/2m_f$ and \hbar is the Planck's constant]. Here we assume that the effective mass of a fermion in a dilute mixture is same as its bare mass [12]. Under the LDA, the densities $n_b(r)$ and $n_f(r)$ in the harmonic trap should satisfy

$$\mu_{f0} = \alpha n_f^{2/3} + \frac{\partial \mathcal{E}_{bf}}{\partial n_f} + \frac{1}{2} m_f \omega_z^2 r^2, \quad (1)$$

$$\mu_{b0} = \frac{d\mathcal{E}_{bb}}{dn_b} + \frac{\partial \mathcal{E}_{bf}}{\partial n_b} + \frac{1}{2} m_b \omega_z^2 r^2, \quad (2)$$

where μ_{f0} and μ_{b0} are the global chemical potentials of fermions and bosons, respectively, referenced to the trap bottom.

For the determination of the boson-fermion scattering length a_{bf} , we use a mean-field expression for the boson-fermion interaction energy $\mathcal{E}_{bf,M} = (2\pi\hbar^2/m_{bf})a_{bf}n_b n_f$ with $m_{bf} = m_b m_f / (m_b + m_f) = (2/3)m$. Since $\mu_{f0} = m\omega_z^2 R_{\uparrow}^2/2$, Eq. (1) gives the relation, $a_{bf}(r) = [\mu_{f0}(1 - r^2/R_{\uparrow}^2) - \alpha n_f^{2/3}] / (3\pi\hbar^2/m n_b)$. We obtained a value for a_{bf} by averaging $a_{bf}(r)$ over a mixed region ($r < R_c$ with $n_{b,f} > 0.1n_0$). Here, n_0 is the reference density defined as $n_0 = (\mu_{f0}/\alpha)^{3/2}$. In this analysis, the non-interacting outer wing provides absolute density calibration [11].

The scattering length ratio a_{bf}/a turns out to be almost constant over the whole range, $700 \text{ G} < B < 780 \text{ G}$ where we could study BF mixtures [Fig. 3(a)]. For even lower magnetic fields, severe heating occurred, probably due to molecular relaxation processes. By averaging a total of 89 measurements, we obtain $a_{bf} = 1.23(3)a$, close

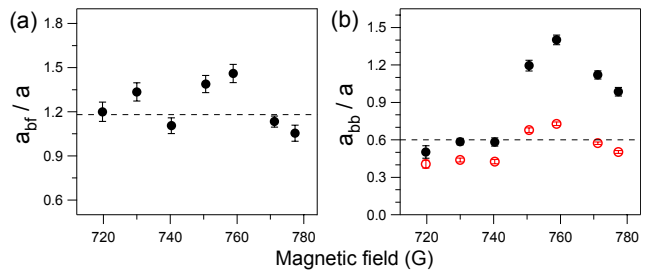


FIG. 3: (color online) Characterization of a strongly interacting Bose-Fermi mixture. (a) The scattering length for dimer-fermion interactions a_{bf} and (b) for dimer-dimer interactions a_{bb} in units of the fermion-fermion scattering length a . Black solid circles were determined using mean-field theory and red open circles including the LHY correction for a strongly interacting Bose gas. The dashed lines indicate the calculated values $a_{bf} = 1.18a$ [4] and $a_{bb} = 0.6a$ [13]. Each data point represents seven to seventeen measurements and the error bars indicate only the statistical uncertainty.

to the exact value $a_{bf} = 1.18a$ calculated for the three-fermion problem [4]. Our finding excludes the mean-field prediction $a_{bf} = (8/3)a$. The detailed behavior above 750 G requires further investigation.

We now turn to the determination of the boson-boson scattering length a_{bb} which parameterizes the boson-boson mean-field energy $\mathcal{E}_{bb,M} = (2\pi\hbar^2/m_b)a_{bb}n_b^2$. For a given a_{bf} , the effective potential for bosons in the presence of fermions is $V_b(r) = m\omega_z^2 r^2 + (3\pi\hbar^2/m)a_{bf}n_f(r)$. Then, Eq. (2) gives $\mu_{b0} - (2\pi\hbar^2/m)a_{bb}n_b(r) = V_b(r)$. By fitting the data in the core region ($0.1R_{\uparrow} < r < R_c$ and $n_b > 0.1n_0$) to this equation with μ_{b0} and a_{bb} as two free parameters, we obtained a value for a_{bb} . We used the value a_{bf} determined from the corresponding profiles.

The effective mean-field values for a_{bb}/a show a strong increase by a factor of about 2, as the system approaches the critical point [Fig. 3(b)]. We attribute this behavior to strong boson-boson interactions causing non-negligible quantum depletion in the BEC. In this regime, the equation of state has to include beyond-mean-field corrections, with the leading term given by Lee, Huang, and Yang (LHY) [5] as

$$\mathcal{E}_{\text{LHY}} = \frac{2\pi\hbar^2 a_{bb} n_b^2}{m_b} \left[1 + \frac{128}{15} \sqrt{\frac{a_{bb}^3 n_b}{\pi}} \right]. \quad (3)$$

Inclusion of the LHY correction leads to smaller fitted values for a_{bb}/a , which are now almost constant over the whole range of magnetic fields with an average value of $a_{bb} = 0.55(1)a$. The exact value for weakly bound dimers is $a_{bb} = 0.6a$ [13]. For $k_{F,b}a = 1$, the LHY correction is $0.3\mathcal{E}_{bb,M}$, i.e. a 30% correction to the mean field approximation. Here, $k_{F,b} = (6\pi^2 n_b)^{1/3}$. Recently, the LHY corrections have been observed via the upshift of collective oscillation frequencies for a strongly interacting BEC [14].

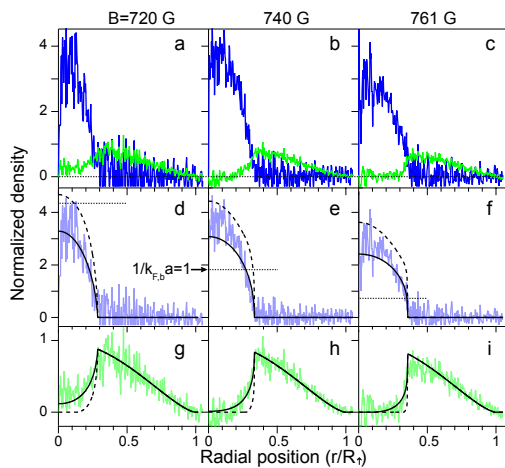


FIG. 4: (color online) Observed profiles of strongly interacting Bose-Fermi mixtures compared to calculated profiles without any adjustable parameter. (a-c) Density profiles of bosonic dimers (blue) and unpaired excess fermions (green) for various magnetic fields. The numerically obtained density profiles (d-f) for bosons and (g-i) for fermions use $a_{bb} = 0.6a$ and $a_{bf} = 1.18a$ (dashed: mean-field description, solid: including the LHY correction). The horizontal dotted lines in (d-f) indicate the boson density corresponding to $1/k_{F,b}a = 1$. The values for T_{F0} (in μK) and R_c/R_\uparrow were respectively: for (a), 1.15 and 0.29; for (b), 1.1 and 0.33; for (c), 1.0 and 0.35.

Our results show that a two-component Fermi mixture beyond the critical point can be effectively described as a strongly interacting BF mixture. In Fig. 4, we compare our experimental data with numerically obtained density profiles [15] without any adjustable parameter, showing excellent agreement. After including the LHY correction, small discrepancies are visible only at the highest boson densities exceeding $k_{F,b}a = 1$, where one would expect unitarity corrections. It is surprising that we didn't need any beyond-mean-field corrections for the boson-fermion interaction. Such corrections have been calculated for a system of point bosons and fermions [16]. However, including them into our fit function degraded the quality of the fit. Recent QMC simulations have shown that the equation of state of a polarized Fermi gas on the BEC side is remarkably close to $\mathcal{E} = \mathcal{E}_{\text{LHY}} + \mathcal{E}_{\text{bf,M}} + \mathcal{E}_f$ with $a_{bb} = 0.6a$ and $a_{bf} = 1.18a$ down to $1/k_{F,\uparrow}a > 0.5$ [8, 17] in agreement with our findings. It appears that the beyond-mean-field term is offset by other corrections, possibly due to the composite nature of the bosons. Further studies of this rich system could address beyond-mean-field terms, characterize the break-down of the BF description close to the critical point, and look for finite temperature effects.

One motivation for the realization of BF mixtures is to extend studies of ^3He - ^4He mixtures. With tunable interactions near Feshbach resonances, cold atom systems can access a wider regime of the phase diagram. Pre-

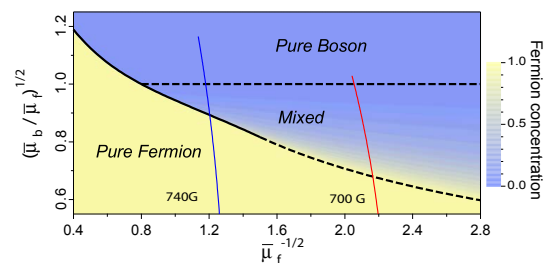


FIG. 5: (color online) Mean-field phase diagram of a dilute Bose-Fermi mixture. $\bar{\mu}_f$ and $\bar{\mu}_b$ are the chemical potentials for fermions and bosons in units of $\frac{\hbar^2}{2m_f}(6\pi^2\bar{n}_f)^{2/3}$ and $\frac{4\pi\hbar^2 a_{bb}}{m_b}\bar{n}_b$, respectively, where $\bar{n}_f = \frac{9\pi}{2} \frac{a_{bb}^3}{a_{bf}^3} \frac{m_b^3 m_f^3}{(m_b+m_f)^6}$ and $\bar{n}_b = \frac{9\pi}{4} \frac{a_{bb}^2}{a_{bf}^5} \frac{m_b^3 m_f^2}{(m_b+m_f)^5}$ (see Ref. [18]). The thick lines indicate the phase transitions (solid: first-order, dashed: second-order). The thin lines represent typical cuts through the phase diagram realized in our trapped samples.

dicted phenomena include phase separation and miscibility [9, 18], boson-mediated, effective fermion-fermion coupling [12, 19] and novel collective excitations [20, 21]. The density profiles in Fig. 4 show a sharper boundary for higher magnetic fields. This is consistent with Fig. 5 which predicts that in the same magnetic field range, the transition from full miscibility to phase separation has taken place.

An interacting BF system has been also realized in ^{87}Rb - ^{40}K mixtures [22, 23]. The ^6Li system studied here has the advantages of using a single atomic species and much longer lifetimes of several seconds, but cannot access attractive boson-fermion interactions.

In conclusion, a two-component Fermi gas with population imbalance is a realization of a long-lived strongly interacting BF mixture. This is a new BF system with tunable interactions. Furthermore, it offers intriguing possibilities to study the emergence of bosonic behavior from a mixture of fermions.

We thank A. Keshet for a critical reading of the manuscript. This work was supported by NSF, ONR, MURI and ARO Award W911NF-07-1-0493 (DARPA OLE Program).

* Electronic address: yishin@mit.edu

- [1] M. W. Zwierlein *et al.*, Science **311**, 492 (2006); M. W. Zwierlein *et al.*, Nature **442**, 54 (2006); Y. Shin *et al.*, Phys. Rev. Lett. **97**, 030401 (2006).
- [2] Y. Shin *et al.*, Nature **451**, 689 (2008).
- [3] P. Pieri and G. C. Strinati, Phys. Rev. Lett. **96**, 150404 (2006); E. Taylor, A. Griffin, and Y. Ohashi, Phys. Rev. A **76**, 023614 (2007); M. Iskin and C. A. R. Sá de Melo, *ibid.* **77**, 013625 (2008).
- [4] G. V. Skorniakov and K. A. Ter-Martirosian, Sov. Phys.

- JETP **4**, 648 (1957).
- [5] T. D. Lee, K. Huang, and C. N. Yang, Phys. Rev. **106**, 1135 (1957).
- [6] M. Bartenstein *et al.*, Phys. Rev. Lett. **94**, 103201 (2005).
- [7] κ is almost independent of the total population imbalance near the resonance [10, 11].
- [8] S. Pilati and S. Giorgini, Phys. Rev. Lett. **100**, 030401 (2008).
- [9] K. Mølmer, Phys. Rev. Lett. **80**, 1804 (1998).
- [10] F. Chevy, Phys. Rev. A **74**, 063628 (2006).
- [11] Y. Shin, Phys. Rev. A **77**, 041603(R) (2008).
- [12] J. Bardeen, G. Baym, and D. Pines, Phys. Rev. **156**, 207 (1967).
- [13] D. S. Petrov, C. Salomon, and G. V. Shlyapnikov, Phys. Rev. Lett. **93**, 090404 (2004).
- [14] A. Altmeyer *et al.*, Phys. Rev. Lett. **98**, 040401 (2007).
- [15] For a given \mathcal{E} , the density profiles were numerically obtained to be self-consistent with Eqs. (1) and (2).
- [16] W. F. Saam, Ann. Phys. **53**, 239 (1969); A. P. Albus *et al.*, Phys. Rev. A **65**, 053607 (2002); L. Viverit and S. Giorgini, *ibid.* **66**, 063604 (2002).
- [17] N. Prokof'ev and B. Svistunov, Phys. Rev. B **77**, 020408(R) (2008).
- [18] L. Viverit, C. J. Pethick, and H. Smith, Phys. Rev. A **61**, 053605 (2000).
- [19] M. J. Bijlsma, B. A. Heringa, and H. T. C. Stoof, Phys. Rev. A **61**, 053601 (2000).
- [20] S. K. Yip, Phys. Rev. A **64**, 023609 (2001).
- [21] D. H. Santamore, S. Gaudio, and E. Timmermans, Phys. Rev. Lett. **93**, 250402 (2004).
- [22] S. Ospelkaus *et al.*, Phys. Rev. Lett. **97**, 120403 (2006).
- [23] M. Zaccanti *et al.*, Phys. Rev. A **74**, 041605(R) (2006).